Synthesis, *in silico* and bio-evaluation studies of new isothiocyanate derivatives with respect to COX inhibition and H_2S release profiles

Yakup Berkay YILMAZ[1], Tuğba GÜNGÖR[2,*], Serhat DÖNMEZ[1], Hazal Nazlıcan ATALAY[1], Pınar SİYAH[3], Serdar DURDAĞI[4,5,6], Mehmet AY[2,*], Tugba BOYUNEGMEZ TUMER[7,*]

[1]Graduate Program of Molecular Biology and Genetics, School of Graduate Studies, Canakkale Onsekiz Mart University, Canakkale, Türkiye

[2]Natural Products and Drug Research Laboratory, Department of Chemistry, Faculty of Science, Canakkale Onsekiz Mart University, Çanakkale, Türkiye

[3]Department of Biochemistry, School of Pharmacy, Bahçeşehir University, Istanbul, Türkiye

[4]Computational Biology and Molecular Simulations Laboratory, Department of Biophysics, School of Medicine, Bahçeşehir University, Istanbul, Türkiye

[5]Molecular Therapy Lab, Department of Pharmaceutical Chemistry, School of Pharmacy, Bahçeşehir University, Istanbul, Türkiye

[6]Lab for Innovative Drugs (Lab4IND), Computational Drug Design Center (HITMER), Bahçeşehir University, Istanbul, Türkiye

[7]Department of Molecular Biology and Genetics, Faculty of Science, Canakkale Onsekiz Mart University, Çanakkale, Türkiye

***Correspondence:** tgungor@comu.edu.tr, mehmetay06@comu.edu.tr, tumertb@comu.edu.tr

Supplementary Data

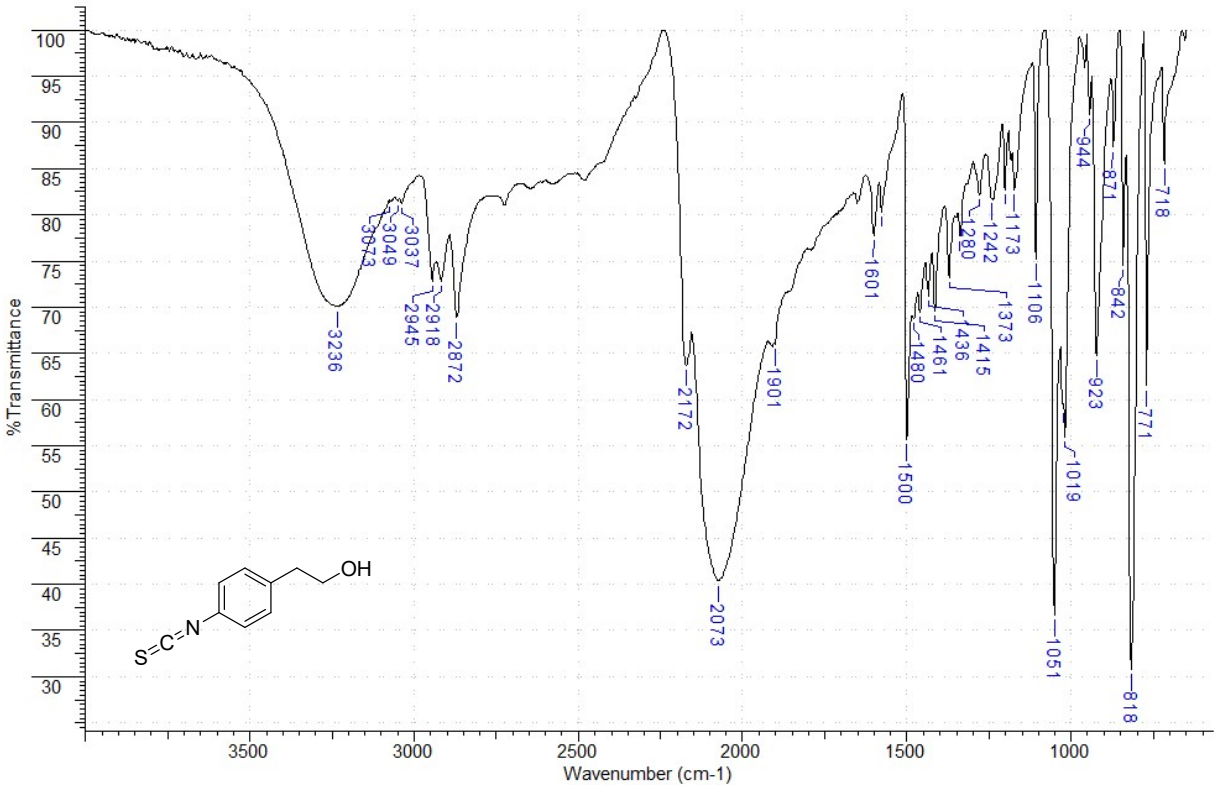

Figure S1. FT-IR spectra of **I1**

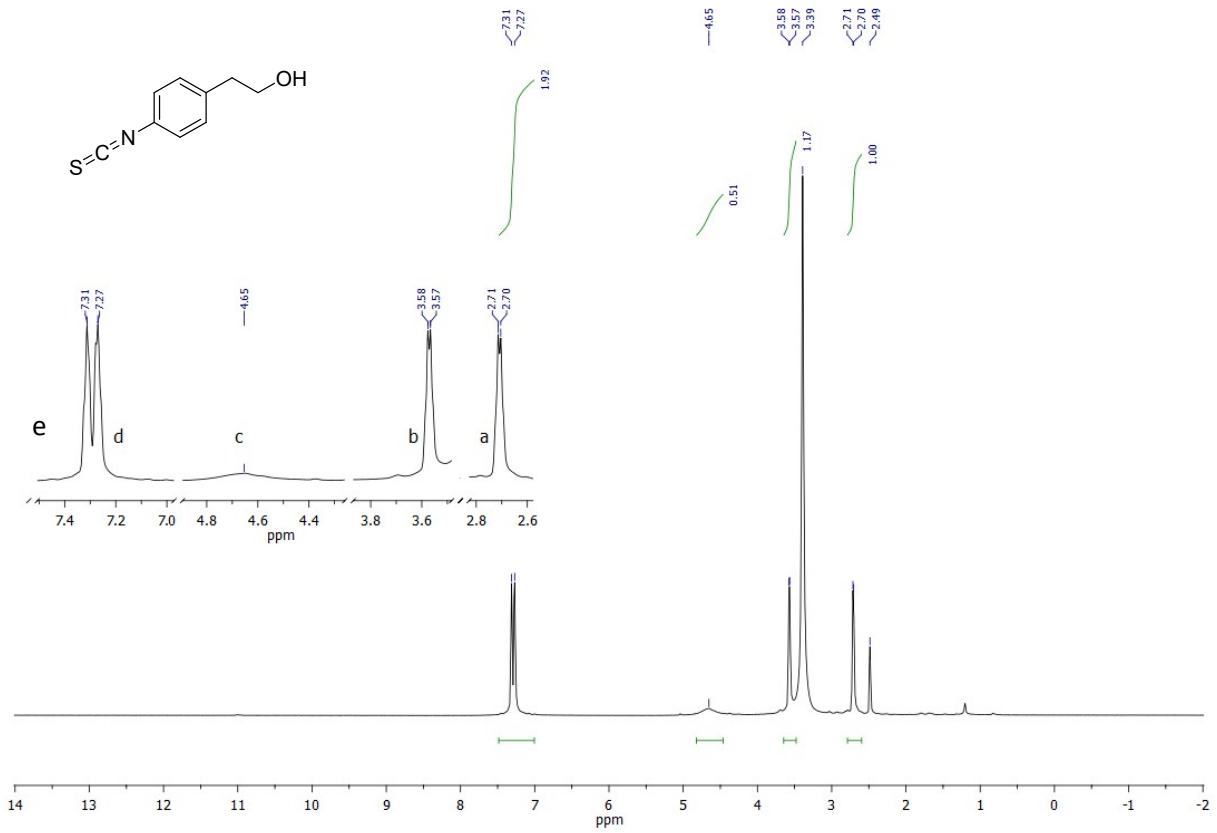

Figure S2. ^{1}H NMR spectra of **I1**

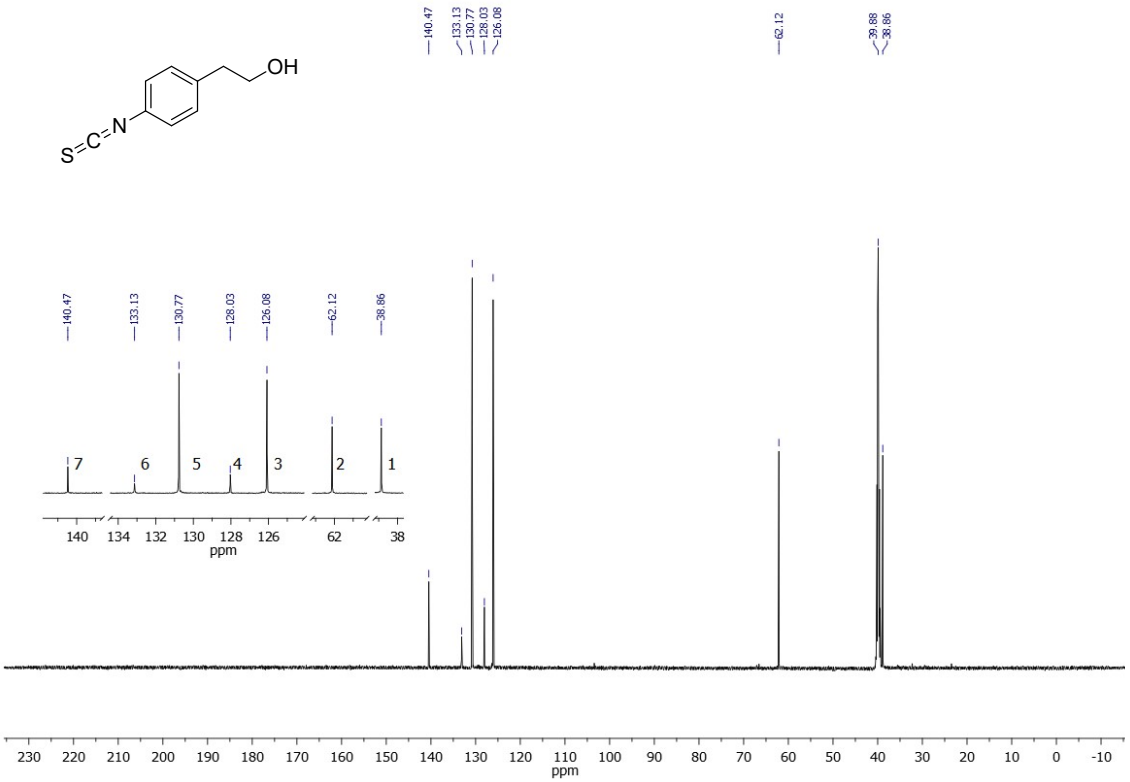

Figure S3. ^{13}C NMR spectra of **I1**

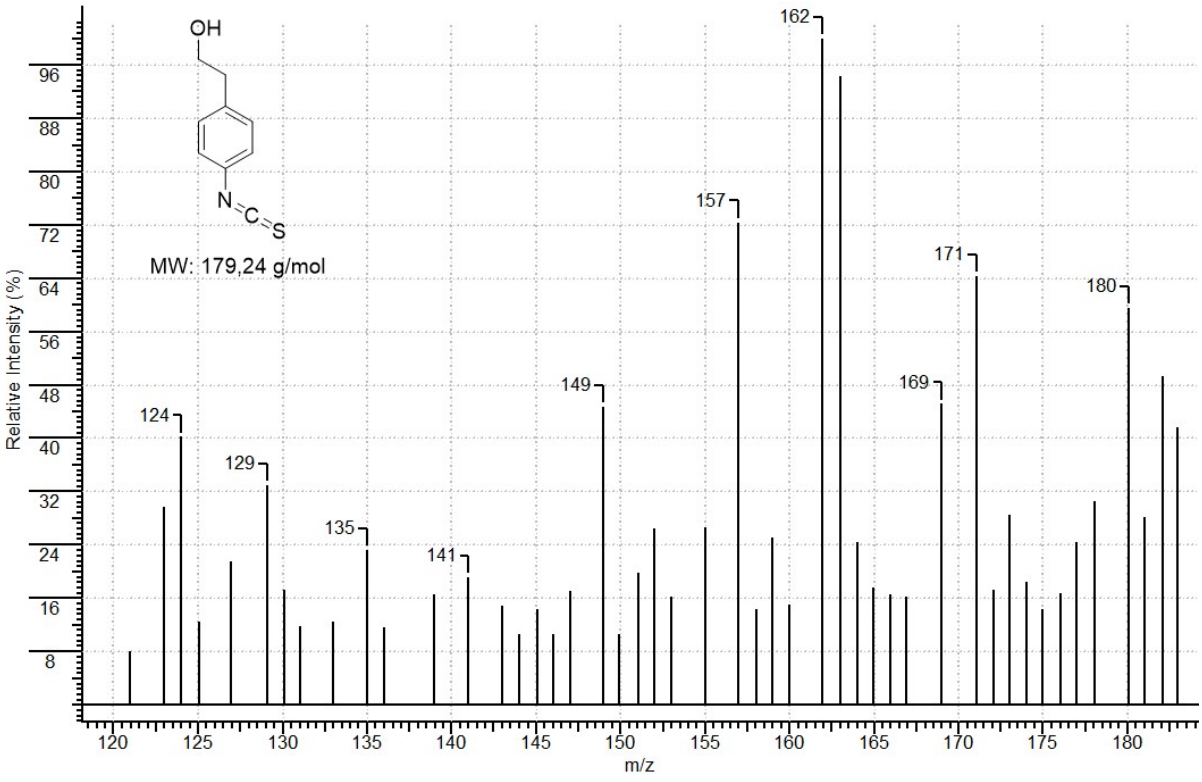

Figure S4. MS spectra of **I1**

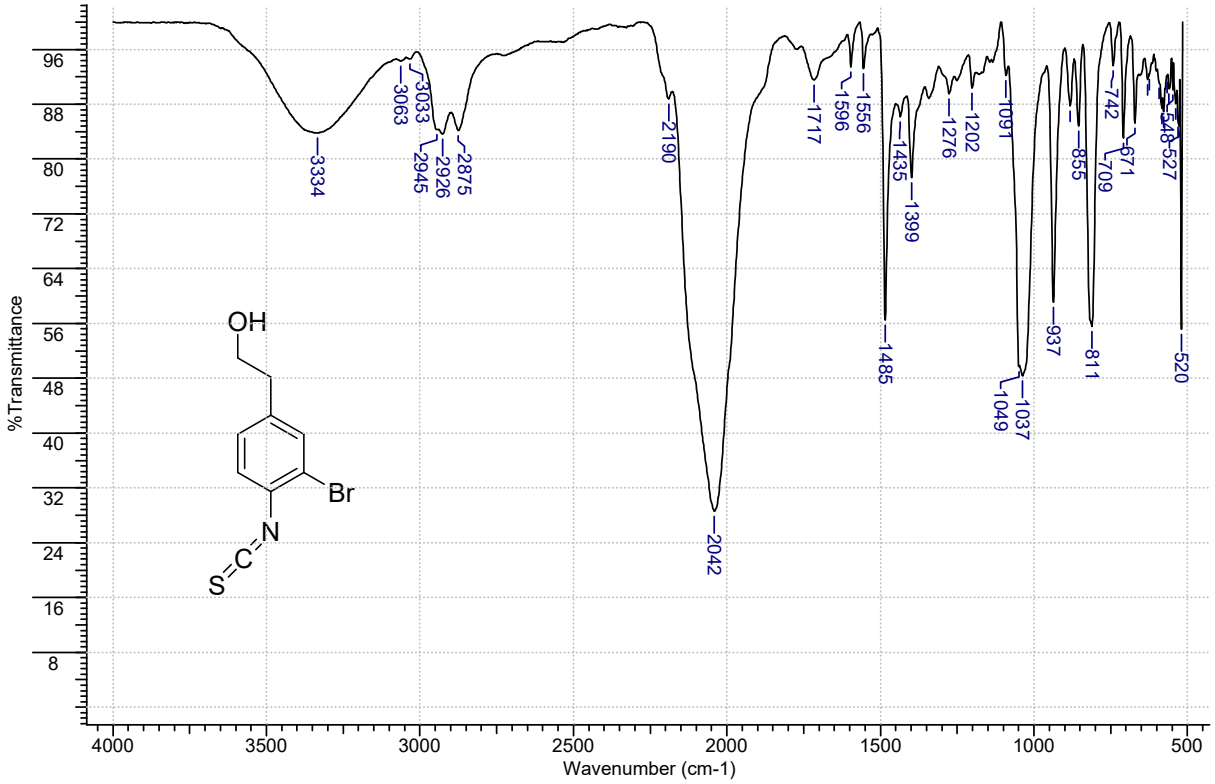

Figure S5. FT-IR spectra of **I2**

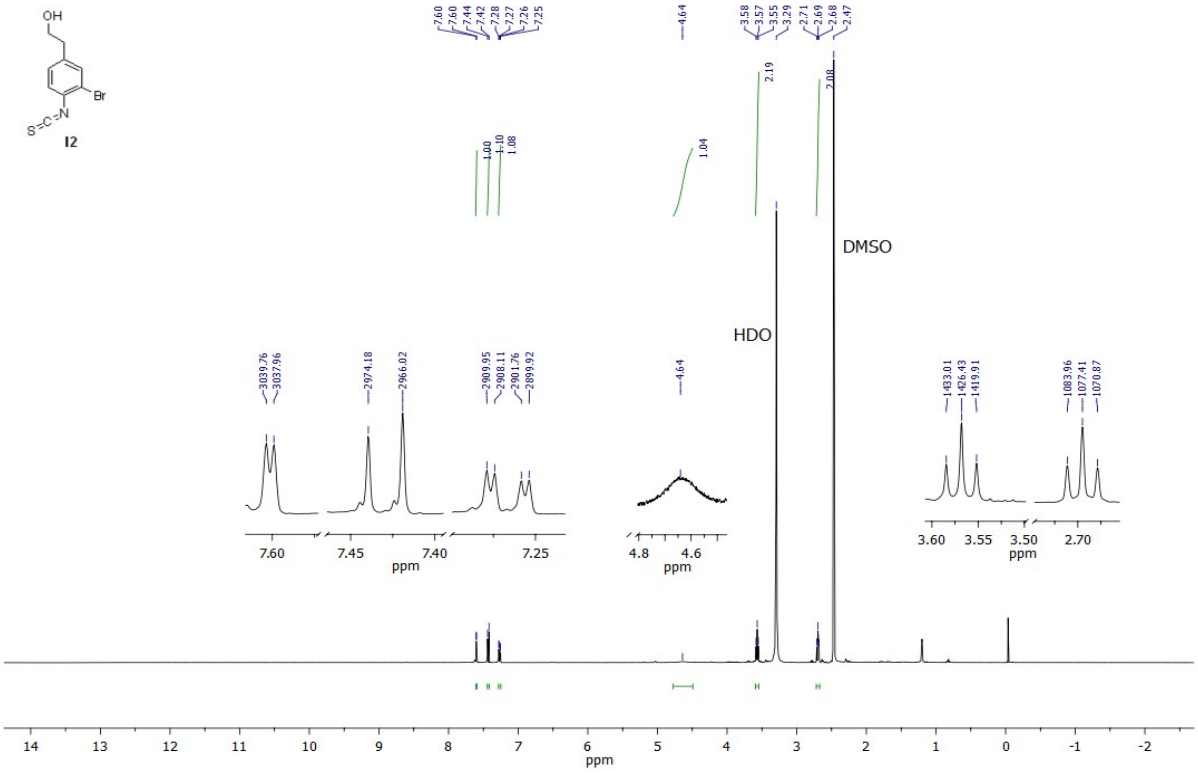

Figure S6. ^{1}H NMR spectra of **I2**

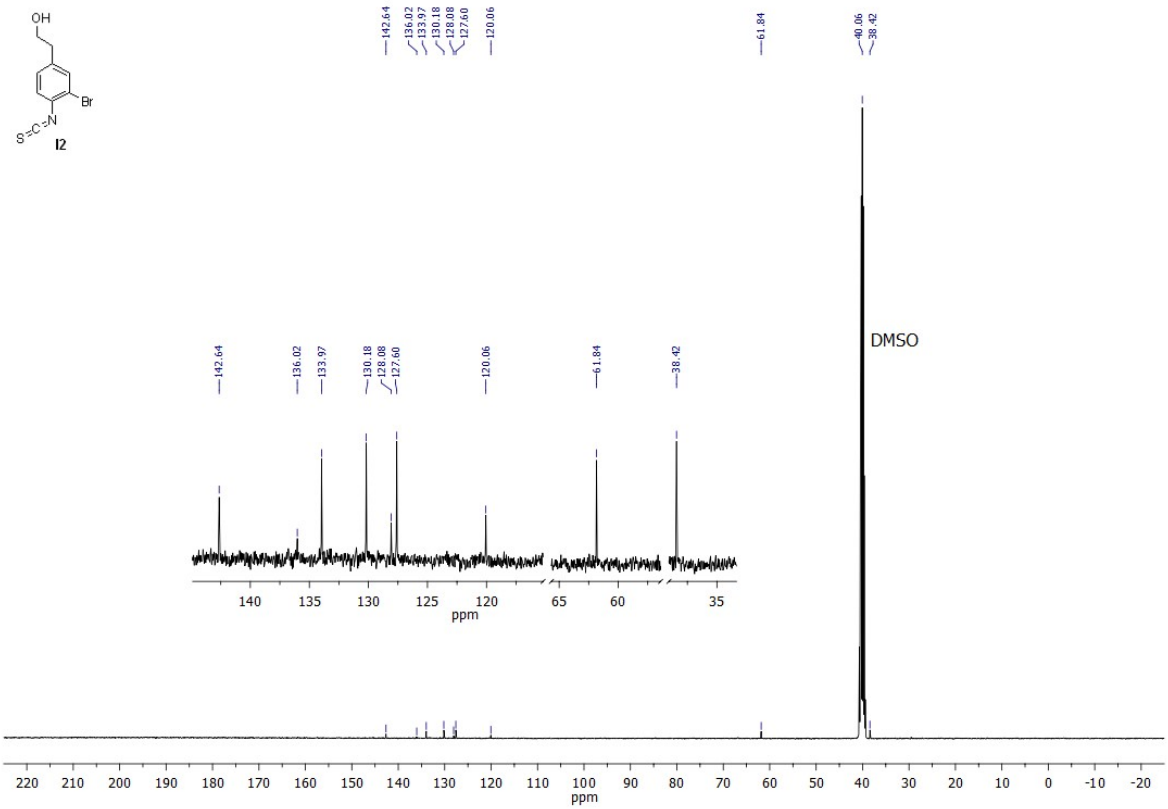

Figure S7. ^{13}C NMR spectra of **I2**

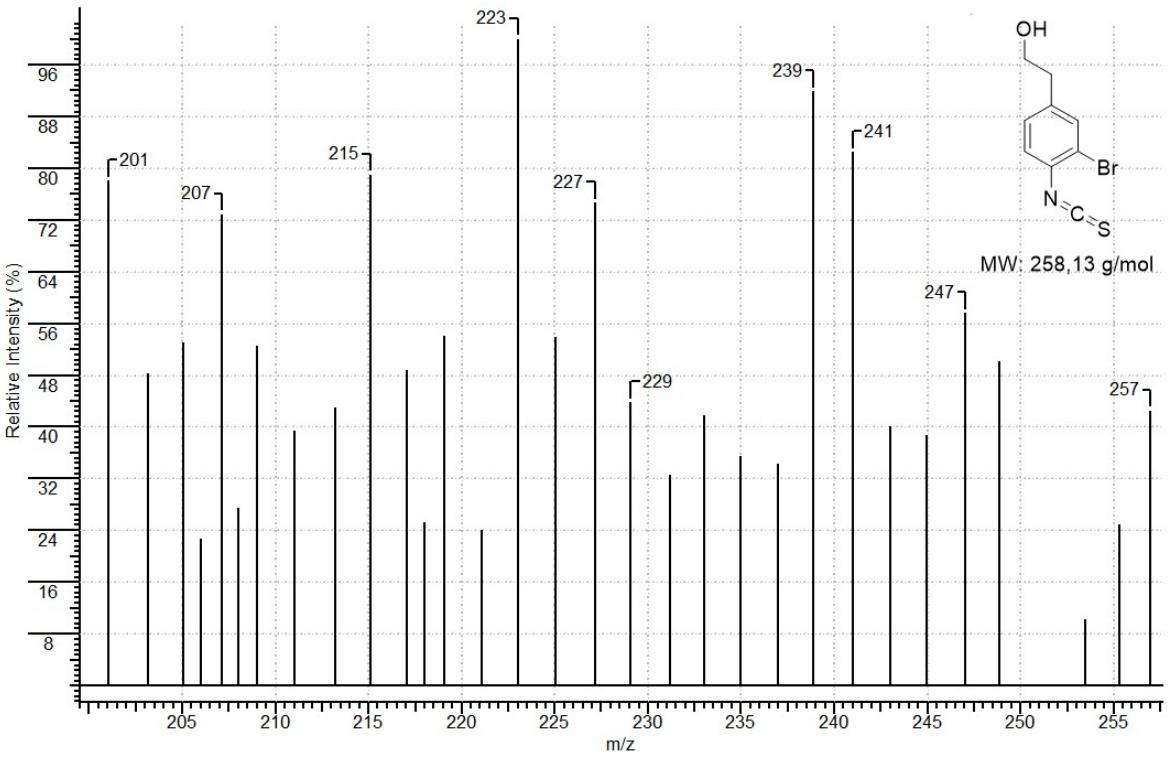

Figure S8. MS spectra of **I2**

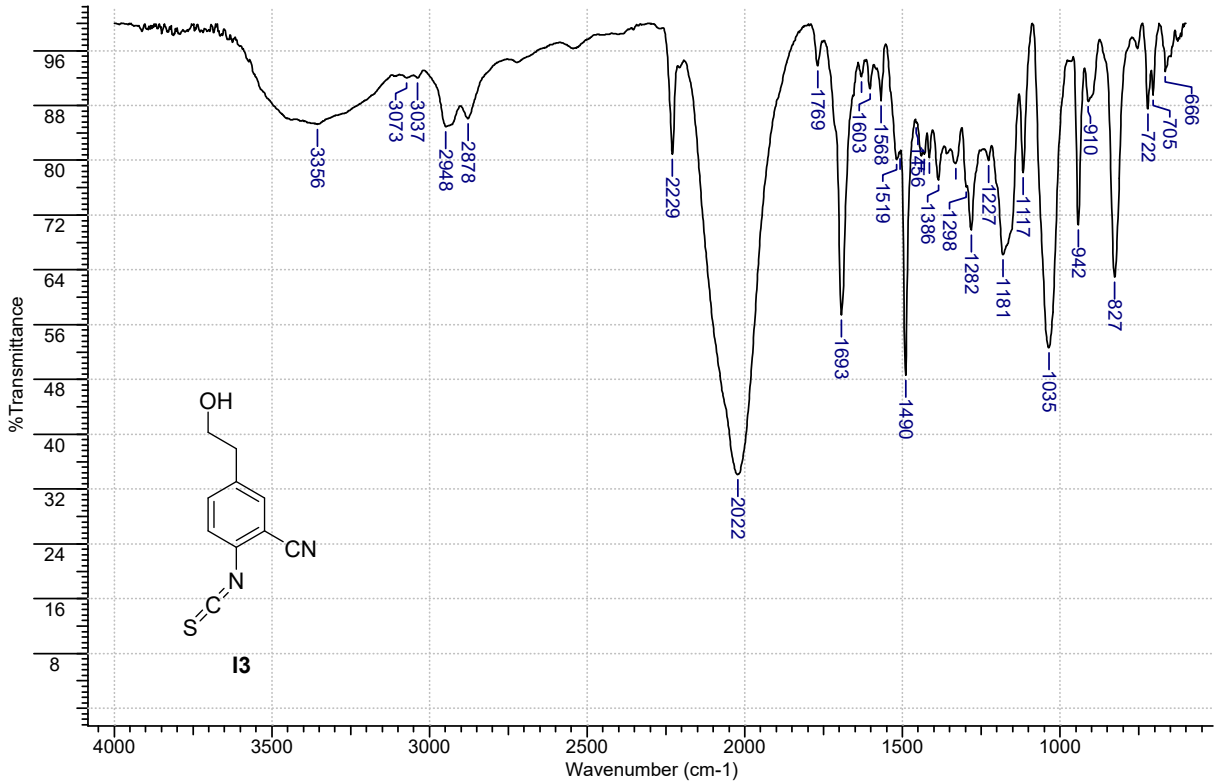

Figure S9. FT-IR spectra of **I3**

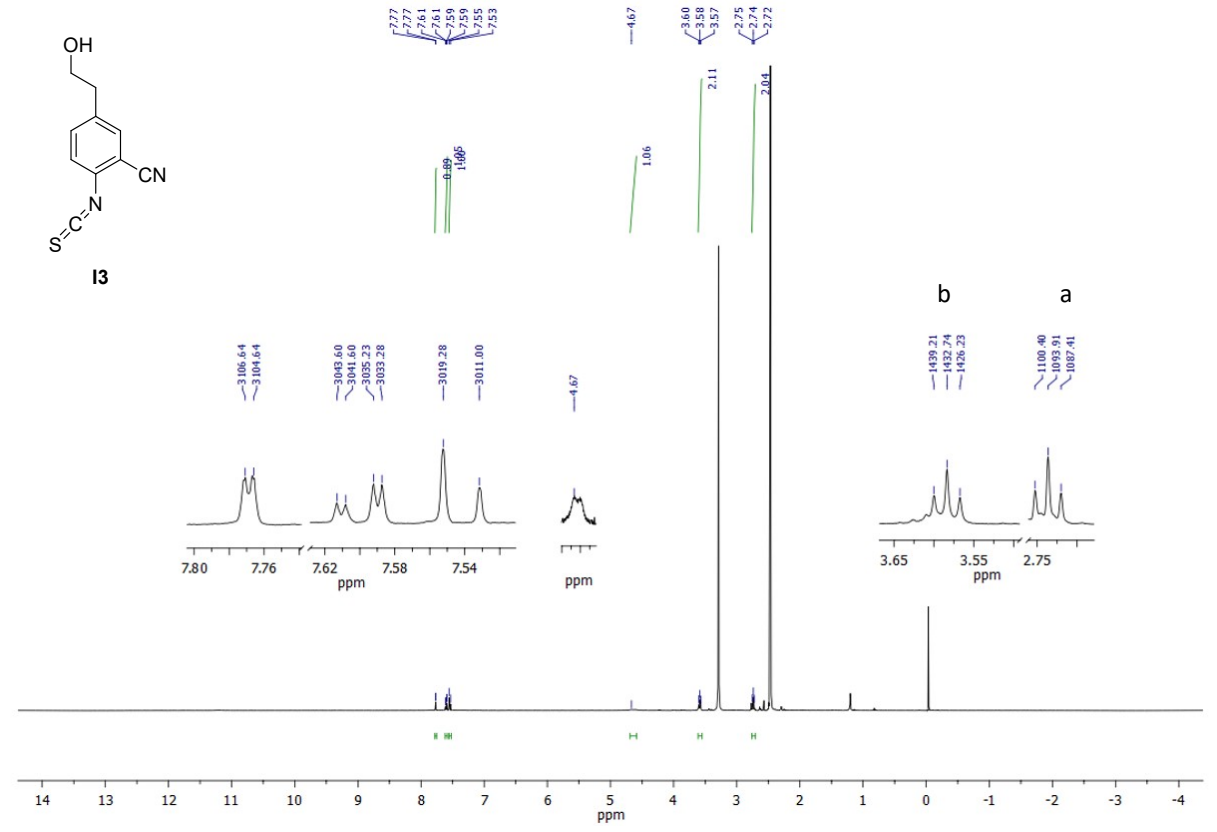

Figure S10. ^{1}H NMR spectra of **I3**

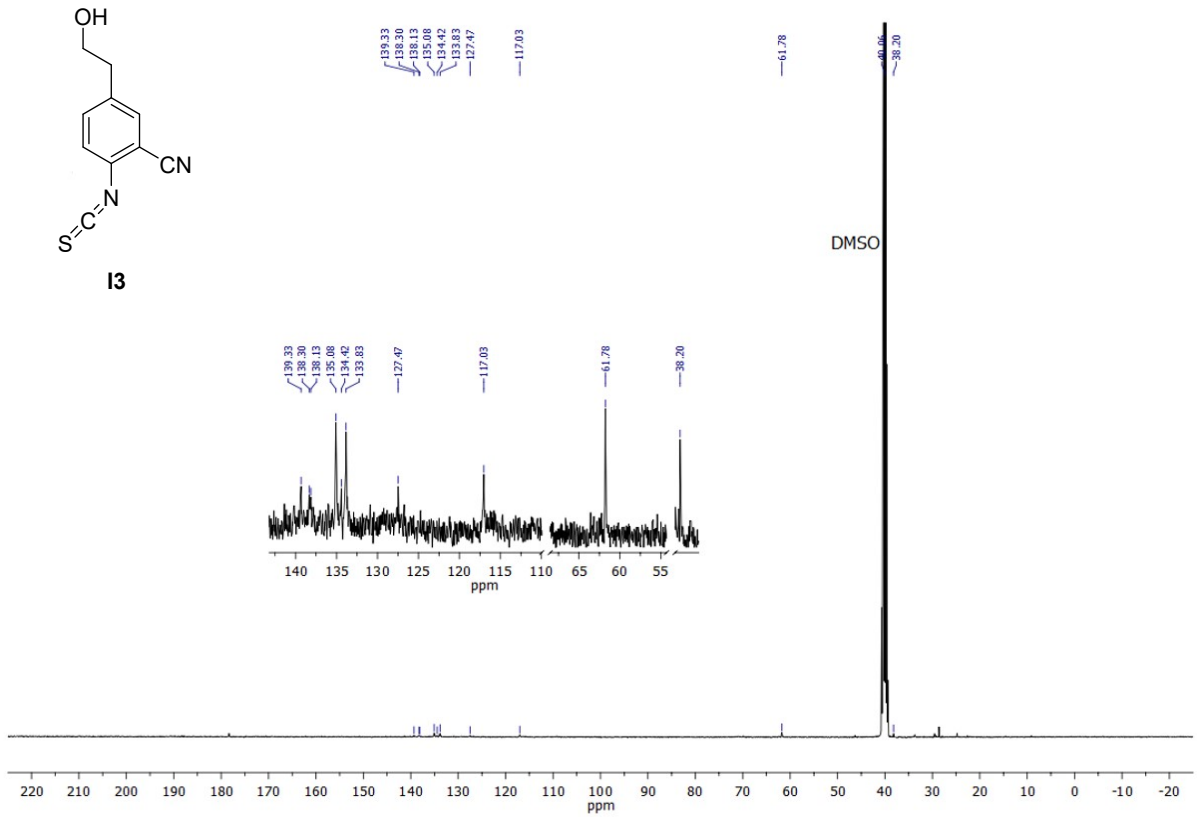

Figure S11. ^{13}C NMR spectra of **I3**

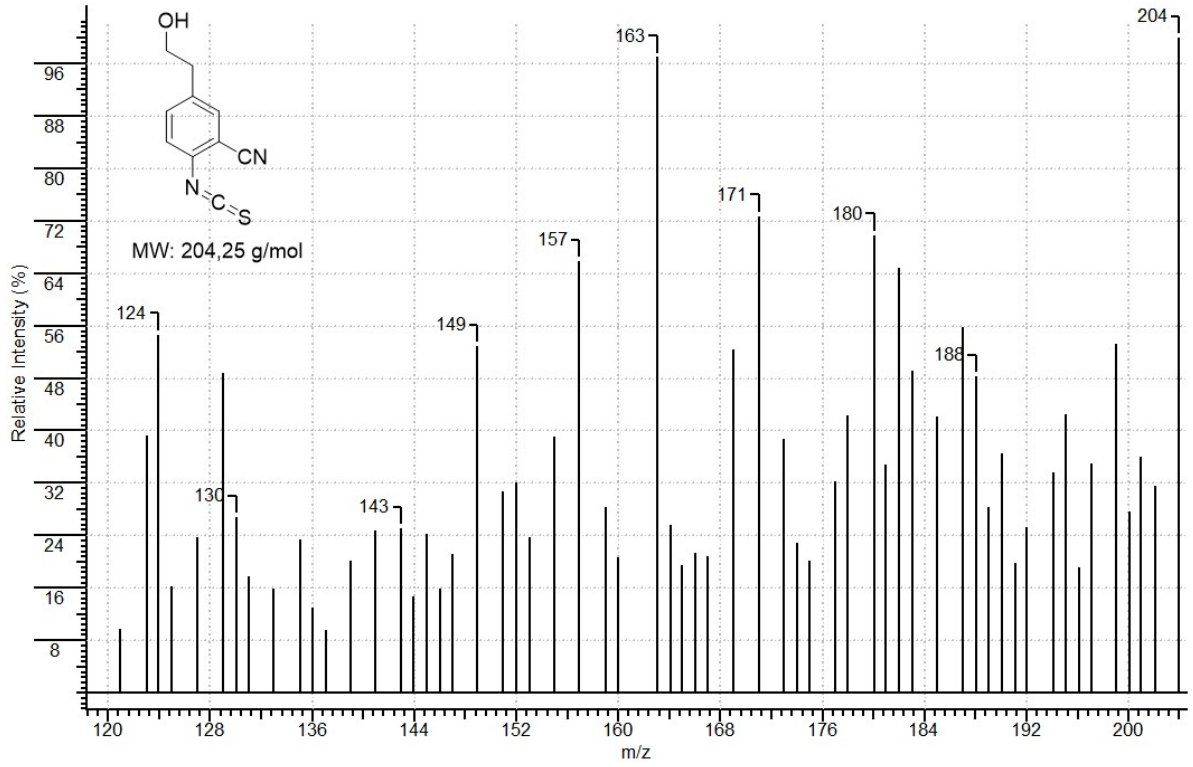

Figure S12. MS spectra of **I3**

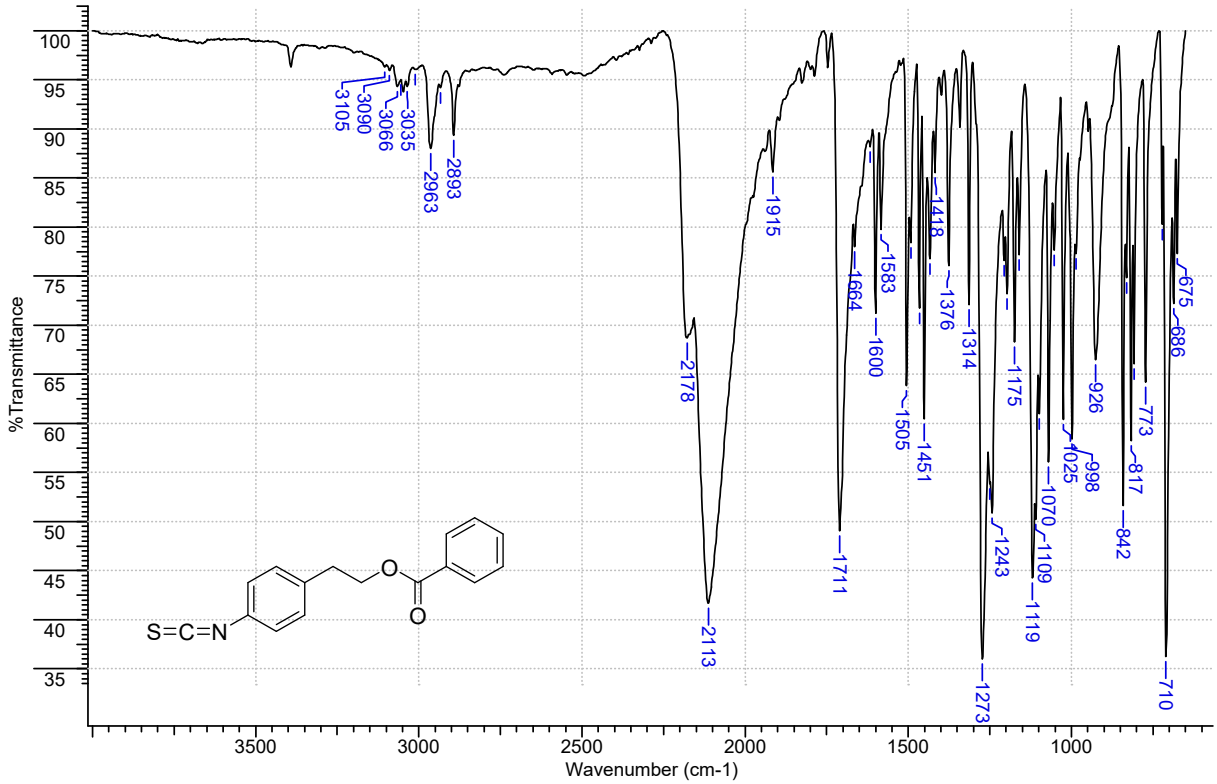

Figure S13. FT-IR spectra of **I1a**

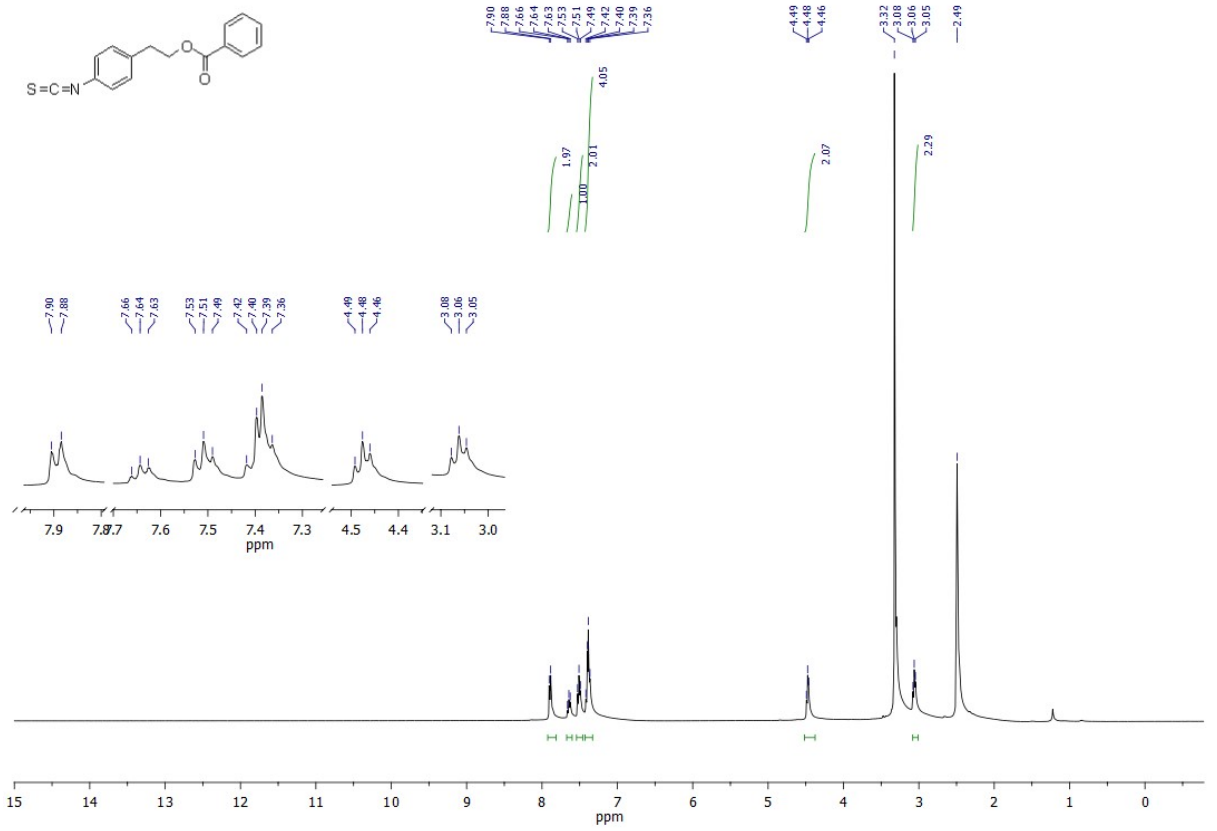

Figure S14. ^{1}H NMR spectra of **I1a**

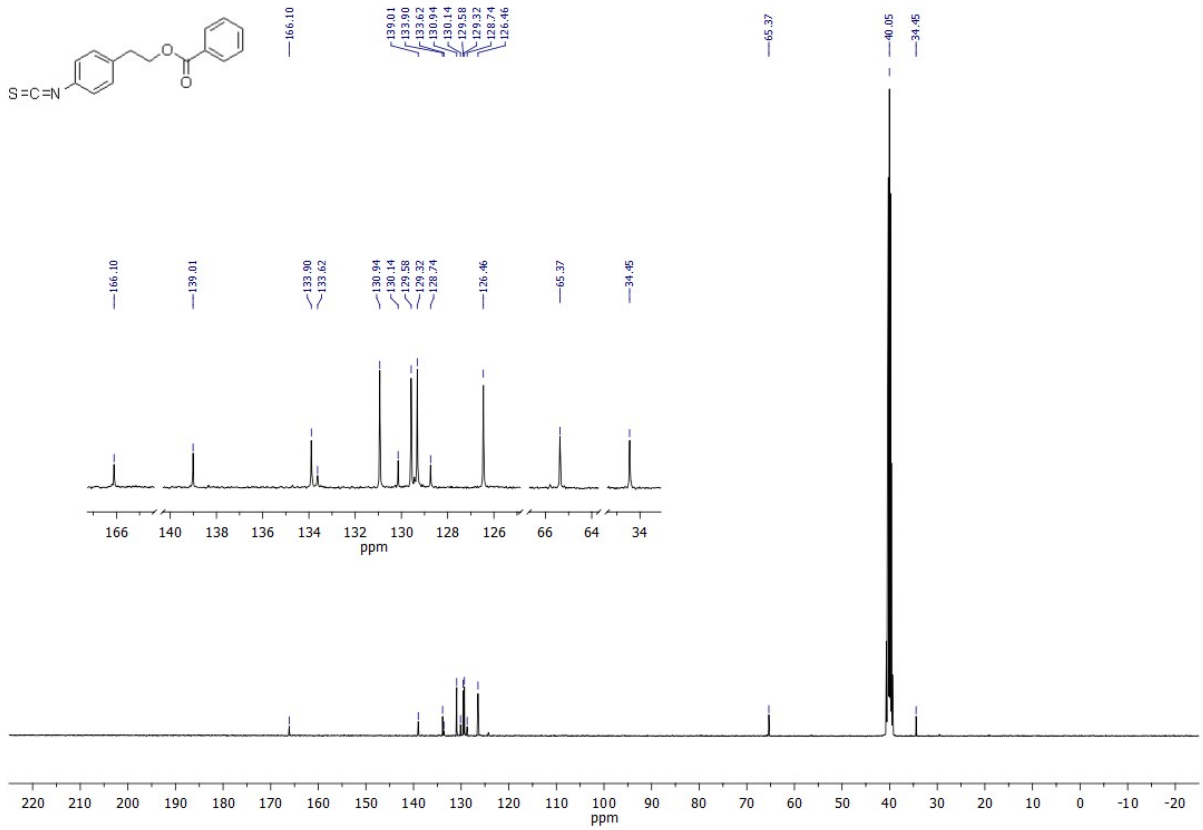

Figure S15. ^{13}C NMR spectra of **I1a**

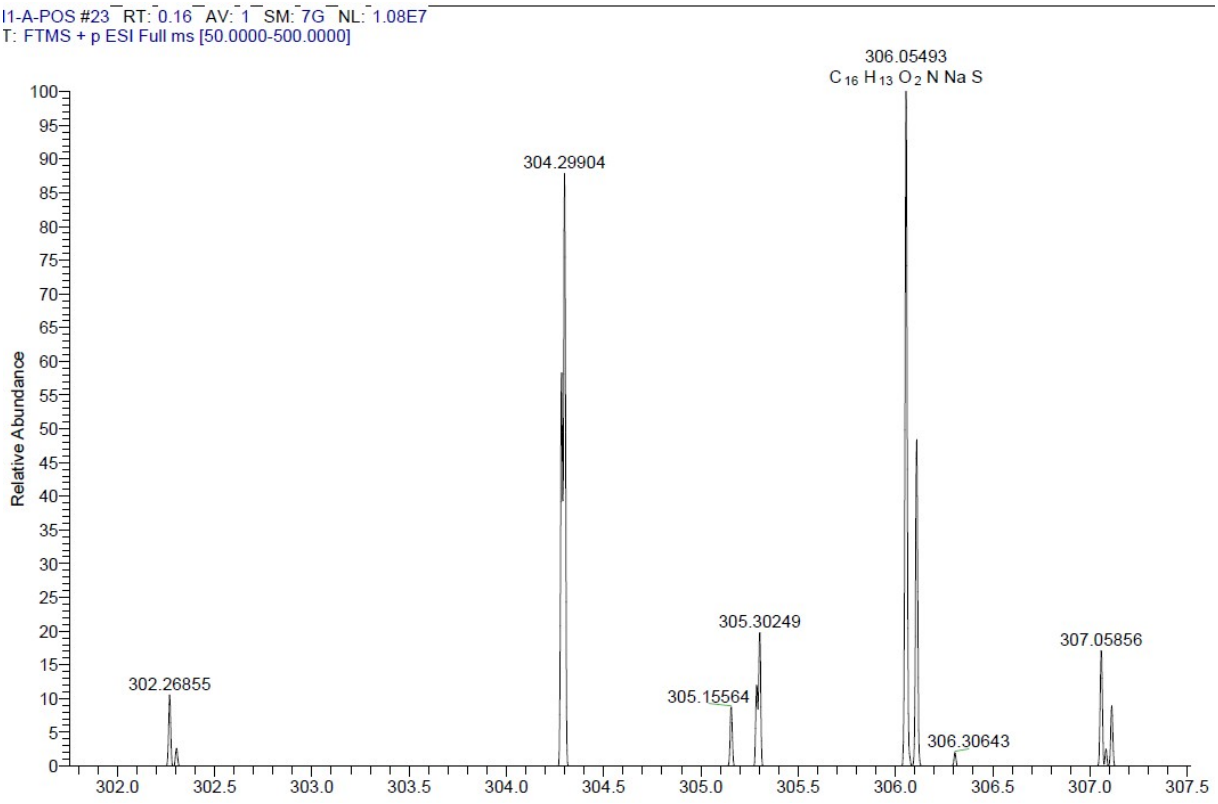

Figure S16. MS spectra of **I1a**

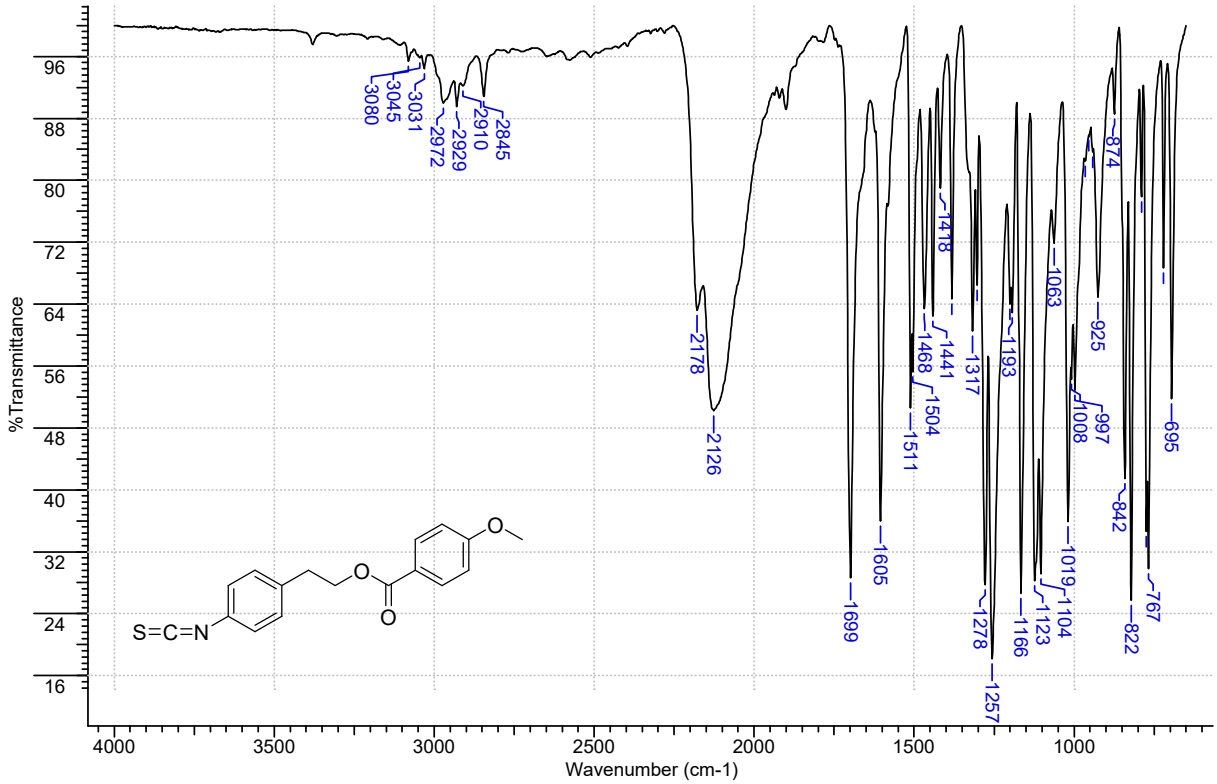

Figure S17. FT-IR spectra of **I1b**

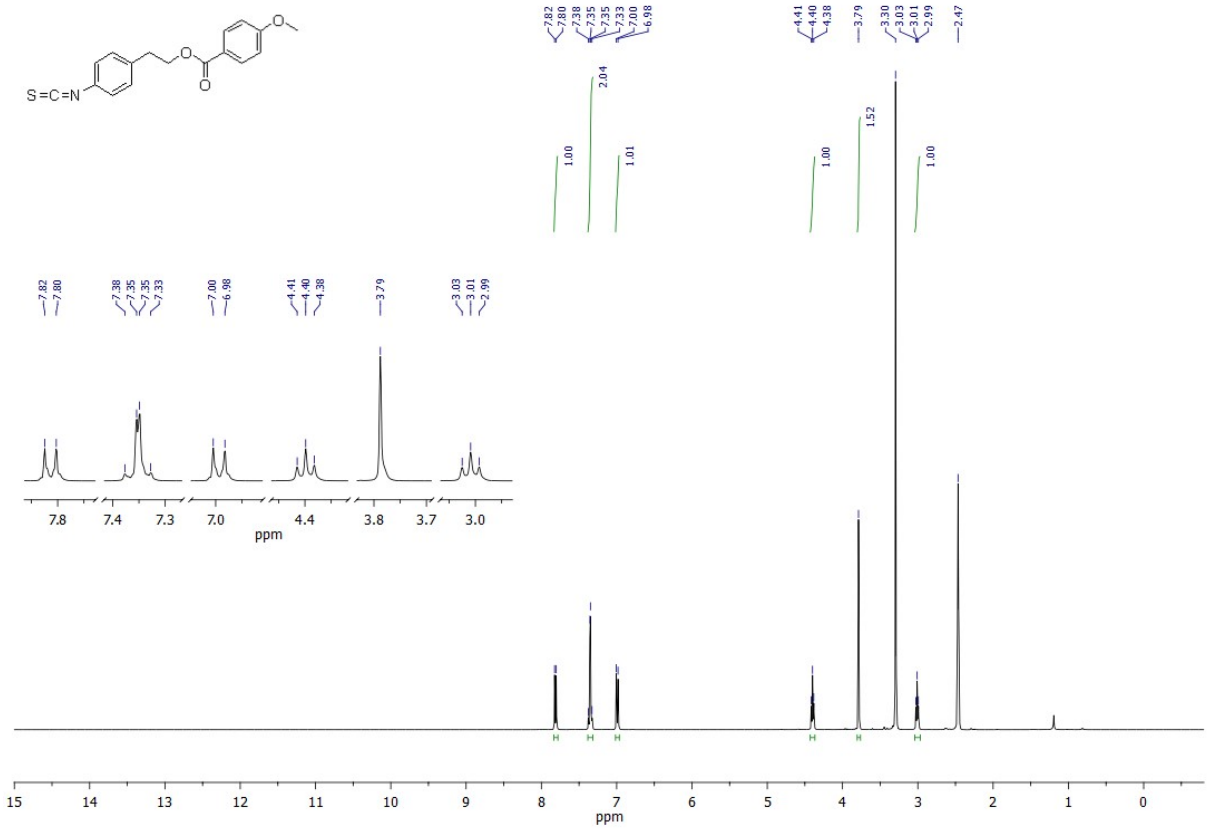

Figure S18. ^{1}H NMR spectra of **I1b**

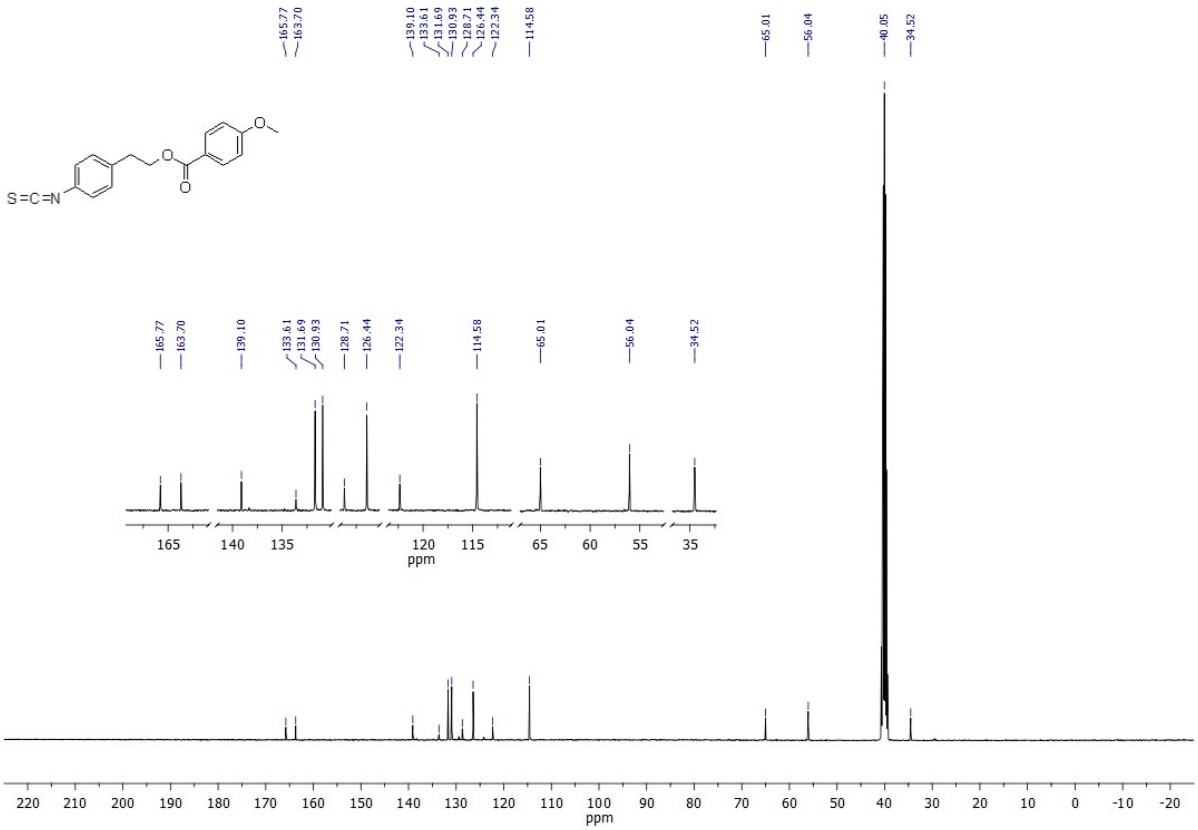

Figure S19. ^{13}C NMR spectra of **I1b**

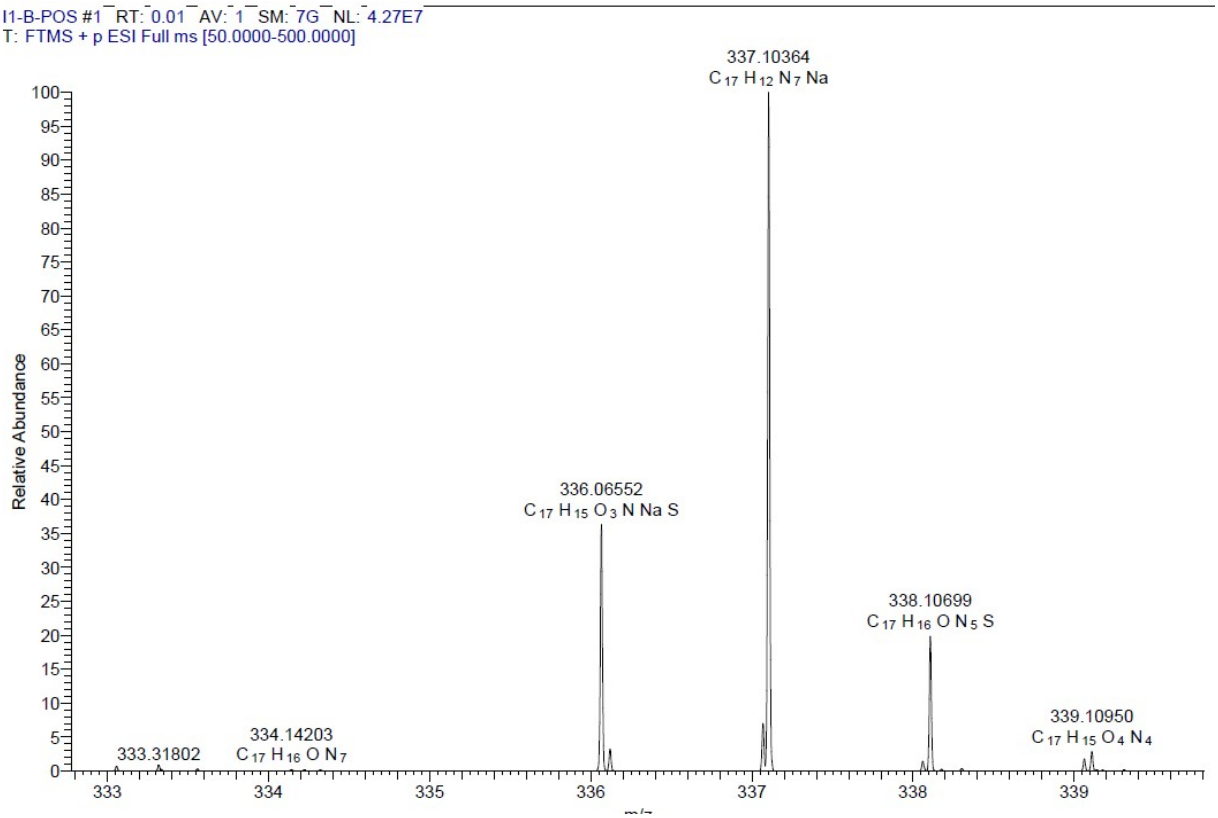

Figure S20. MS spectra of **I1b**

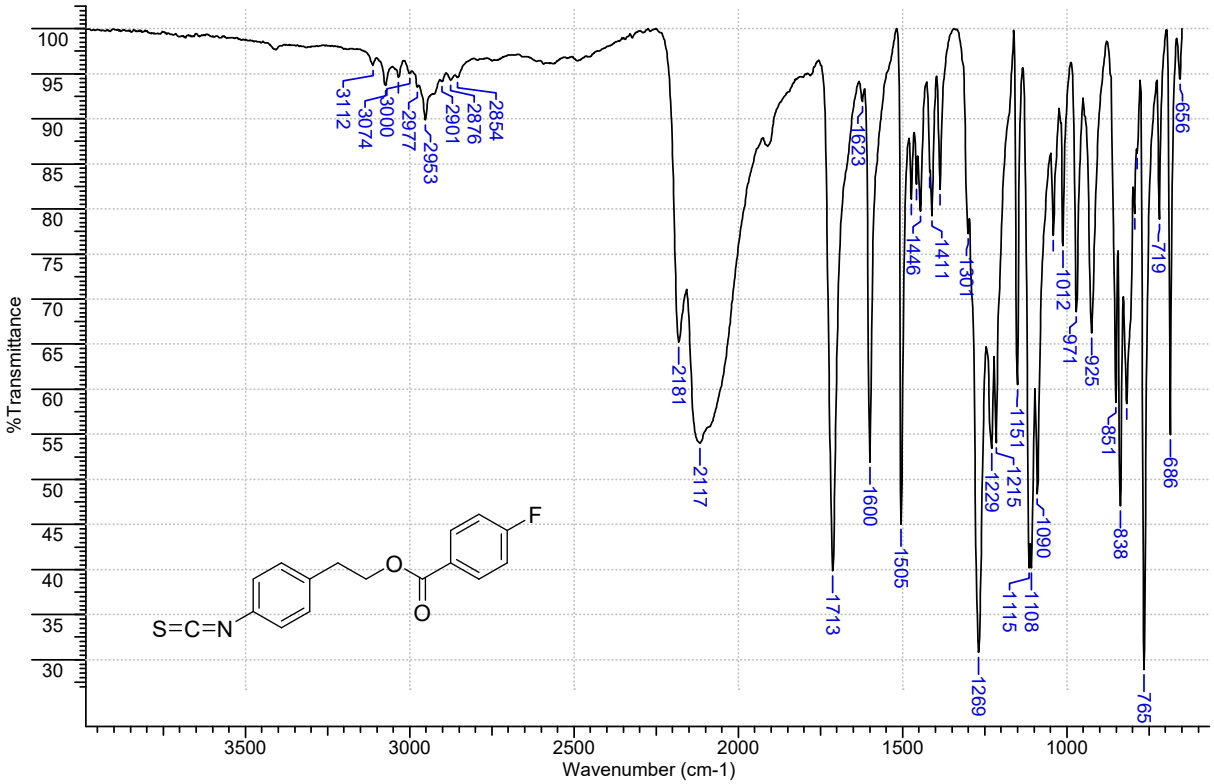

Figure S21. FT-IR spectra of **I1c**

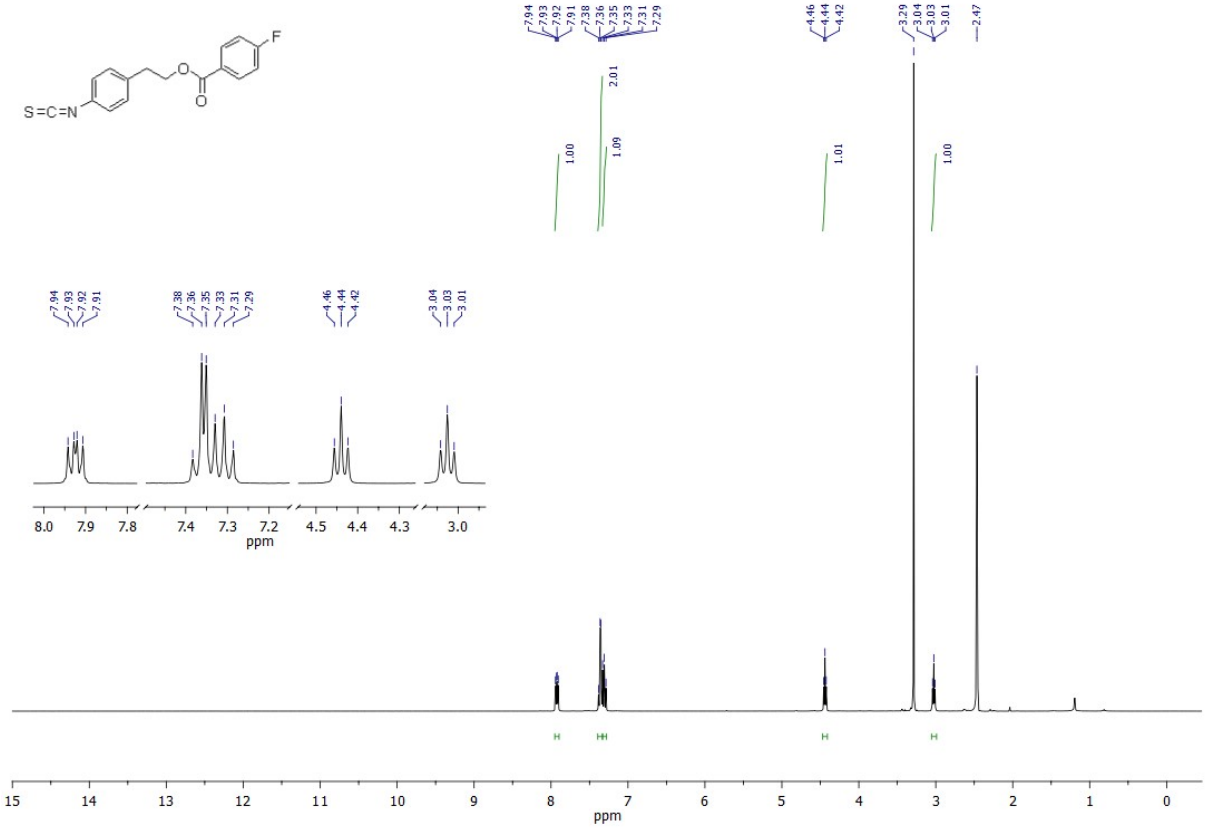

Figure S22. ^{1}H NMR spectra of **I1c**

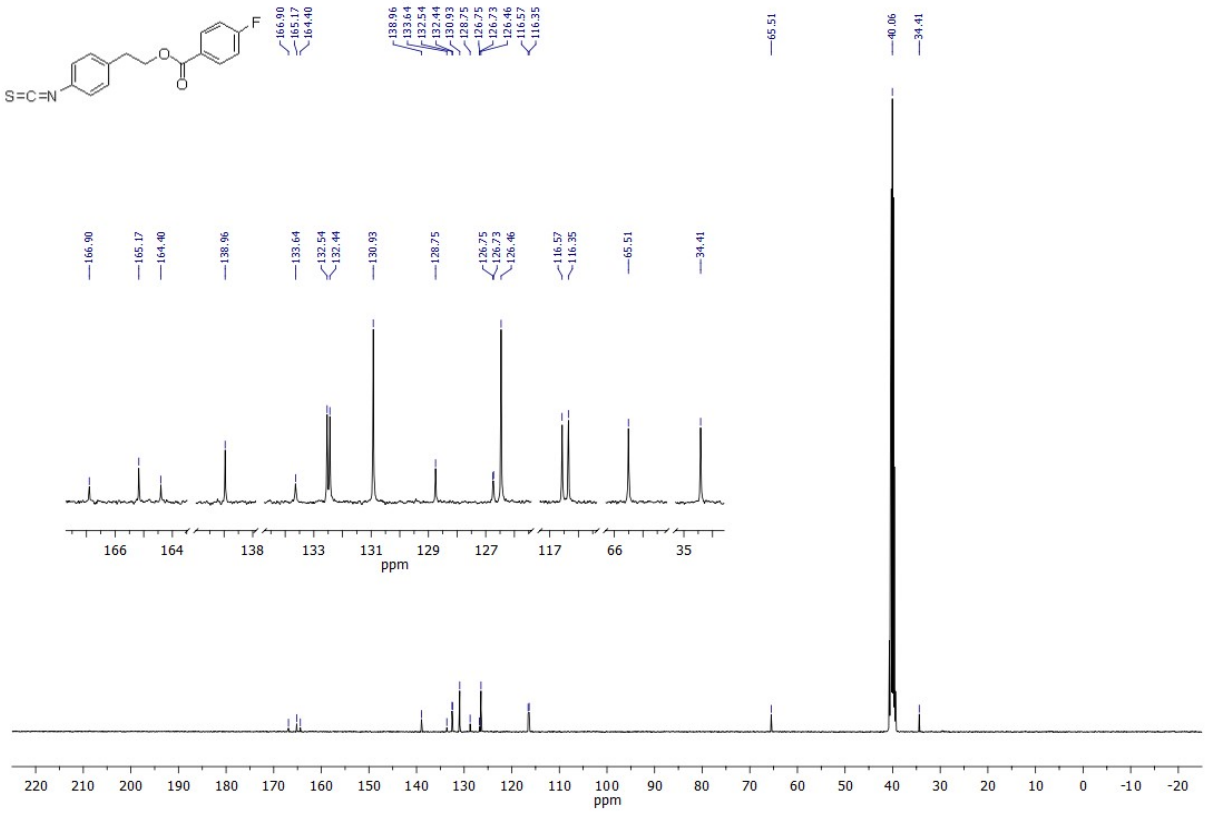

Figure S23. ^{13}C NMR spectra of **I1c**

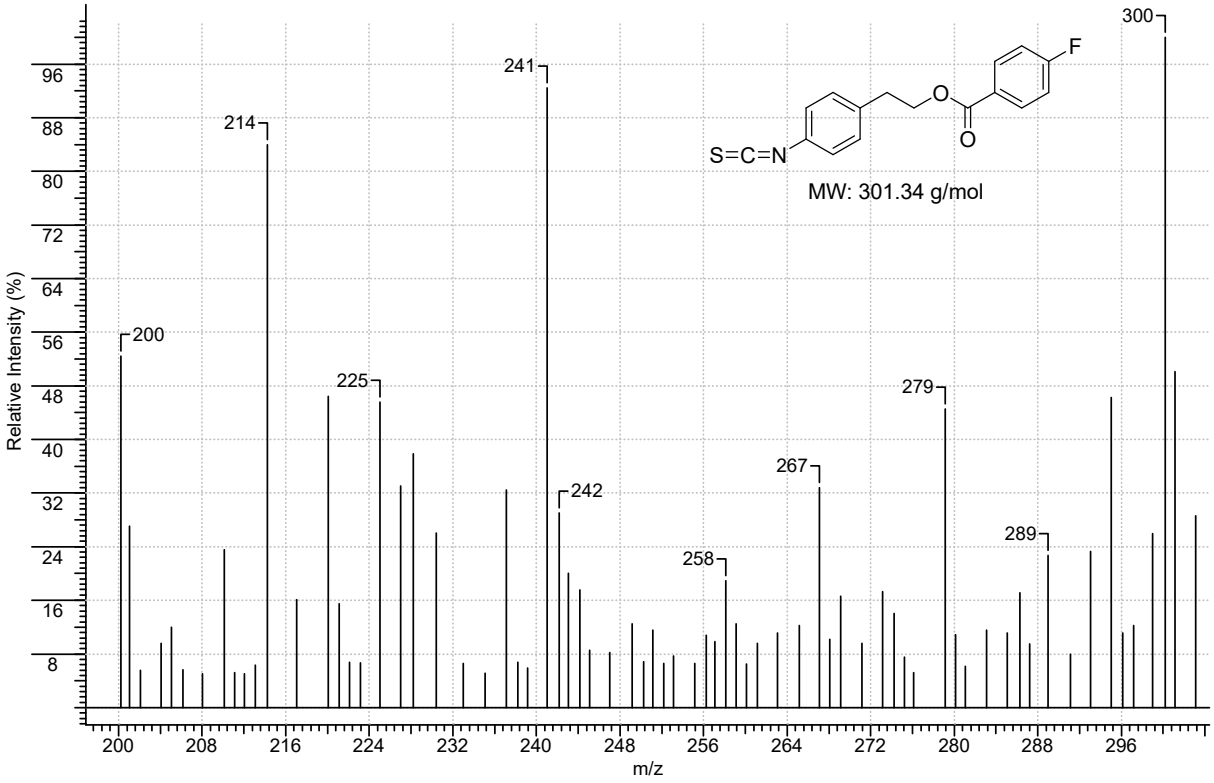

Figure S24. MS spectra of **I1c**

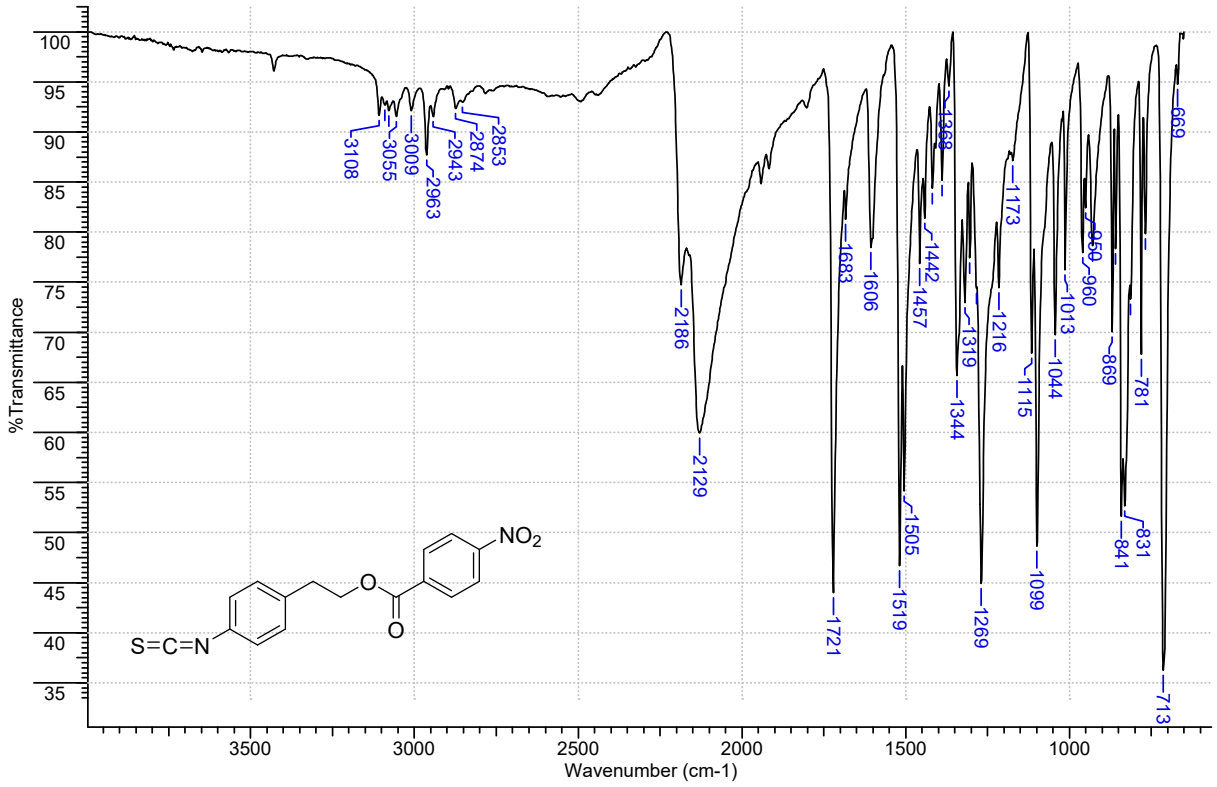

Figure S25. FT-IR spectra of **I1d**

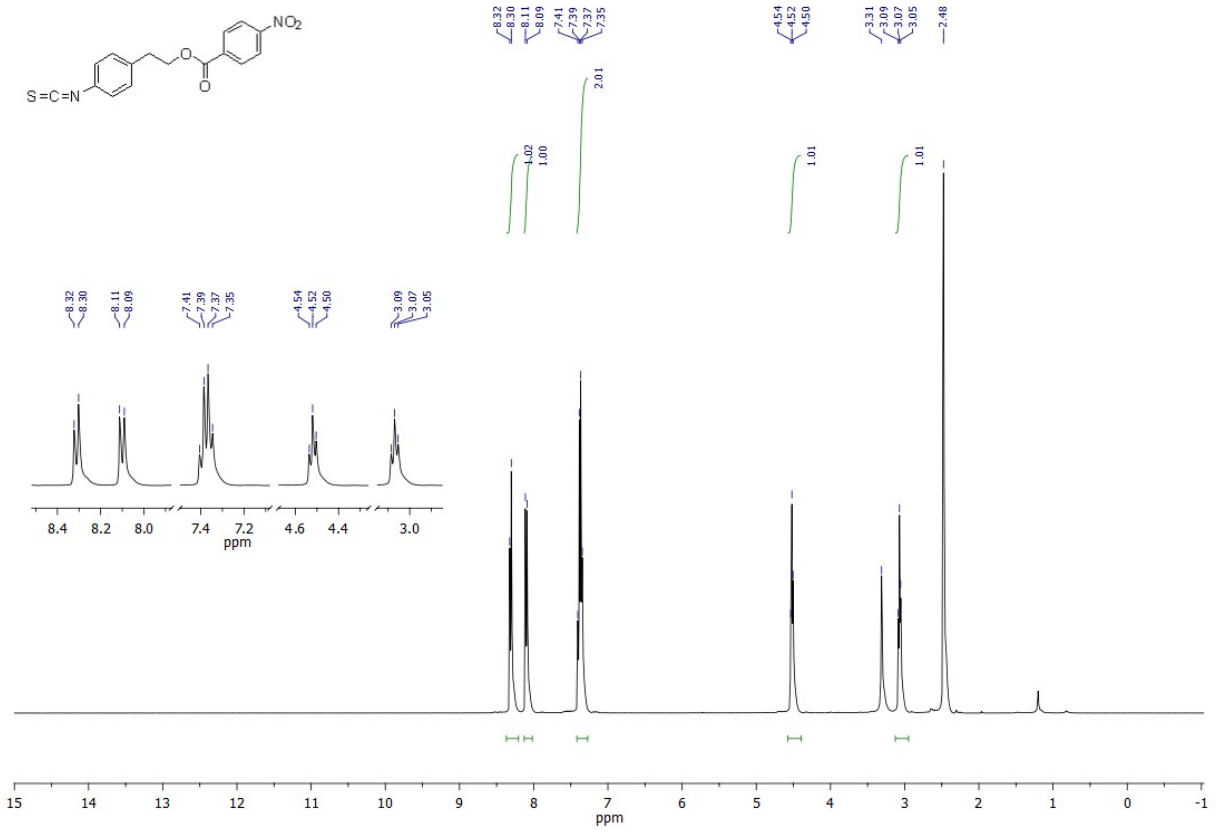

Figure S26. ^{1}H NMR spectra of **I1d**

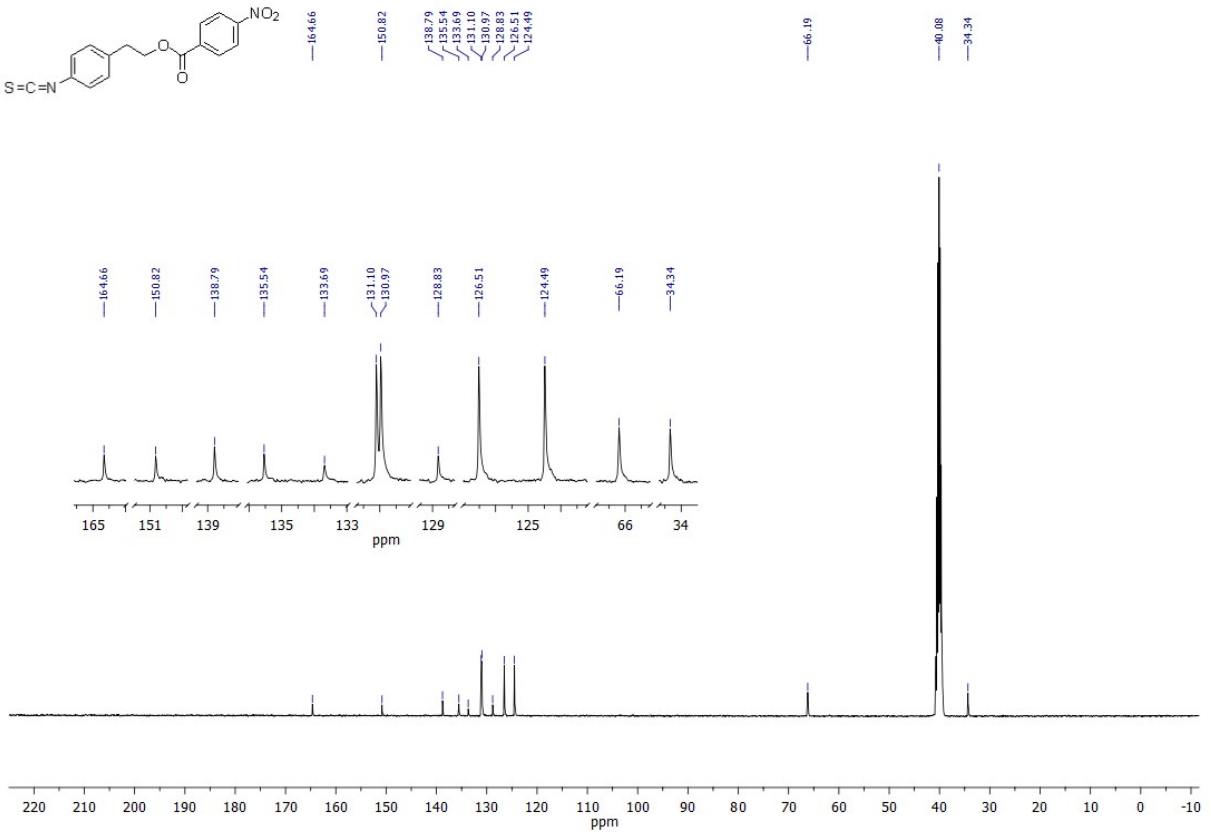

Figure S27. ^{13}C NMR spectra of **I1d**

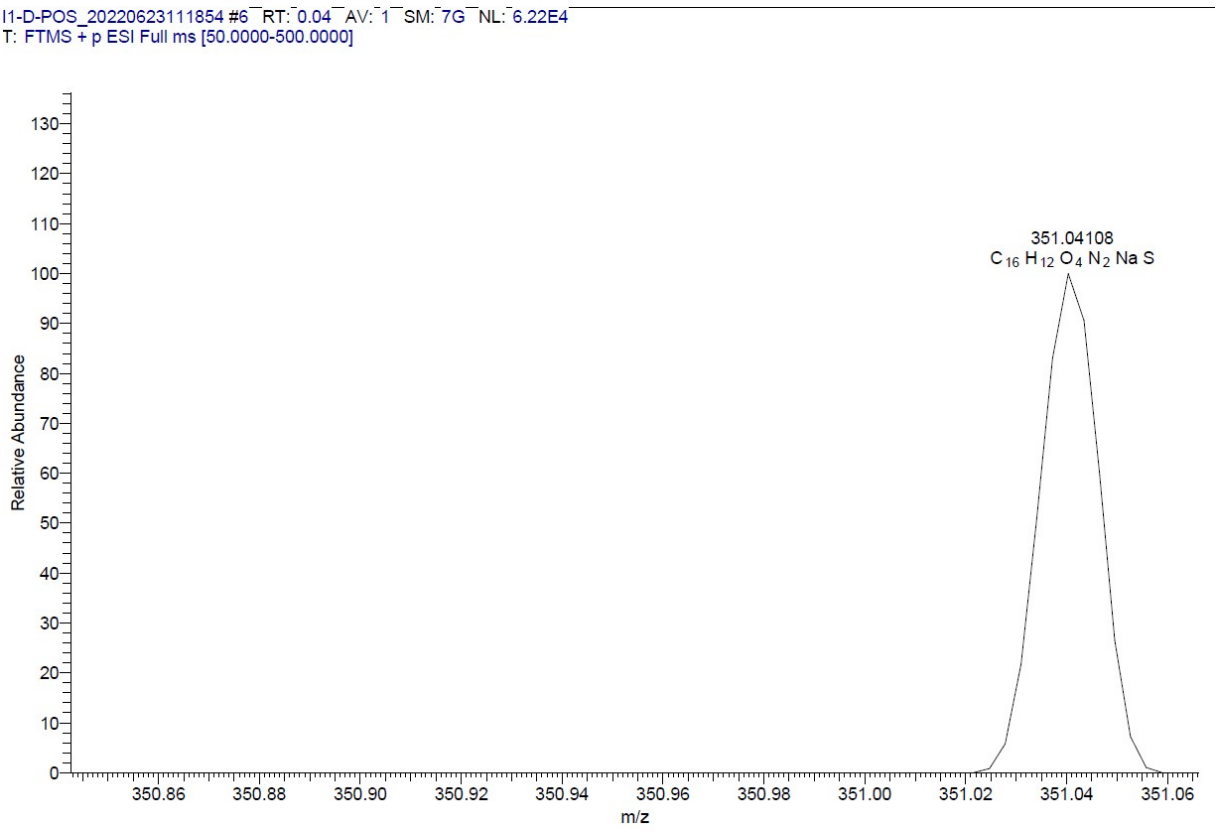

Figure S28. MS spectra of **I1d**

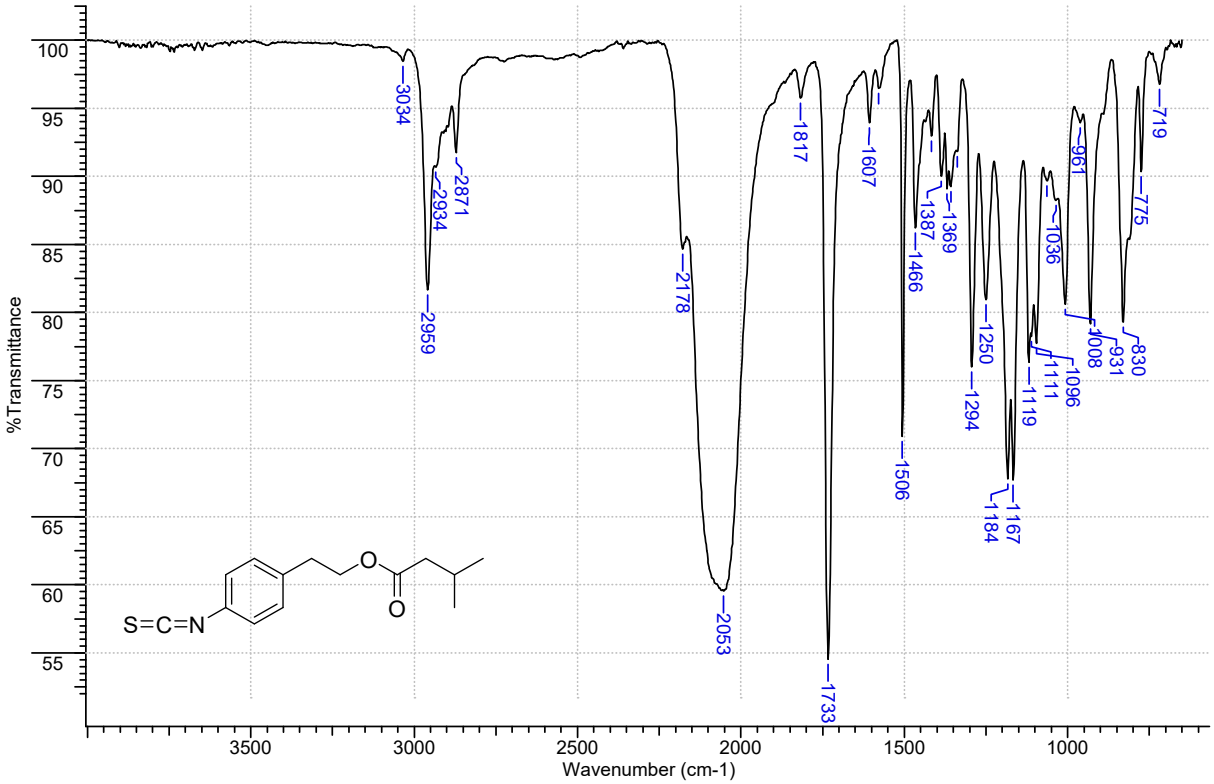

Figure S29. FT-IR spectra of **I1e**

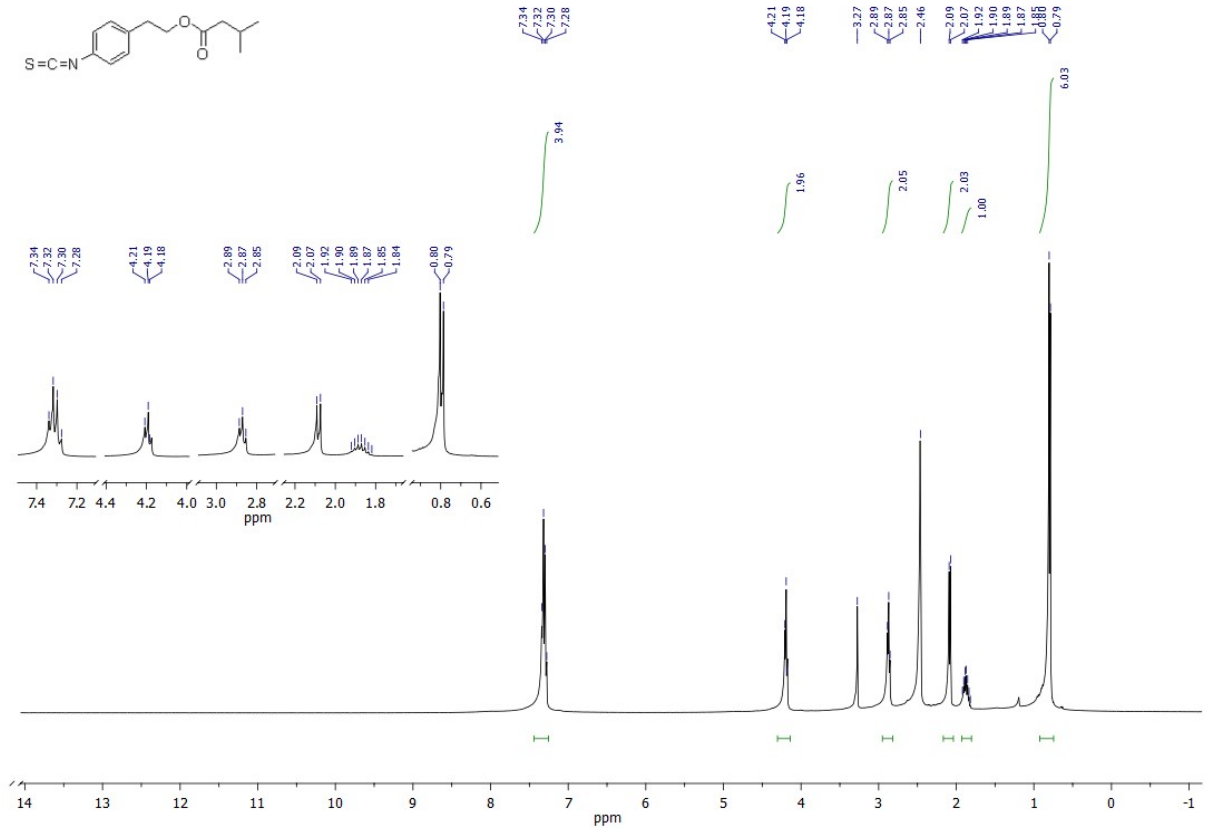

Figure S30. ^{1}H NMR spectra of **I1e**

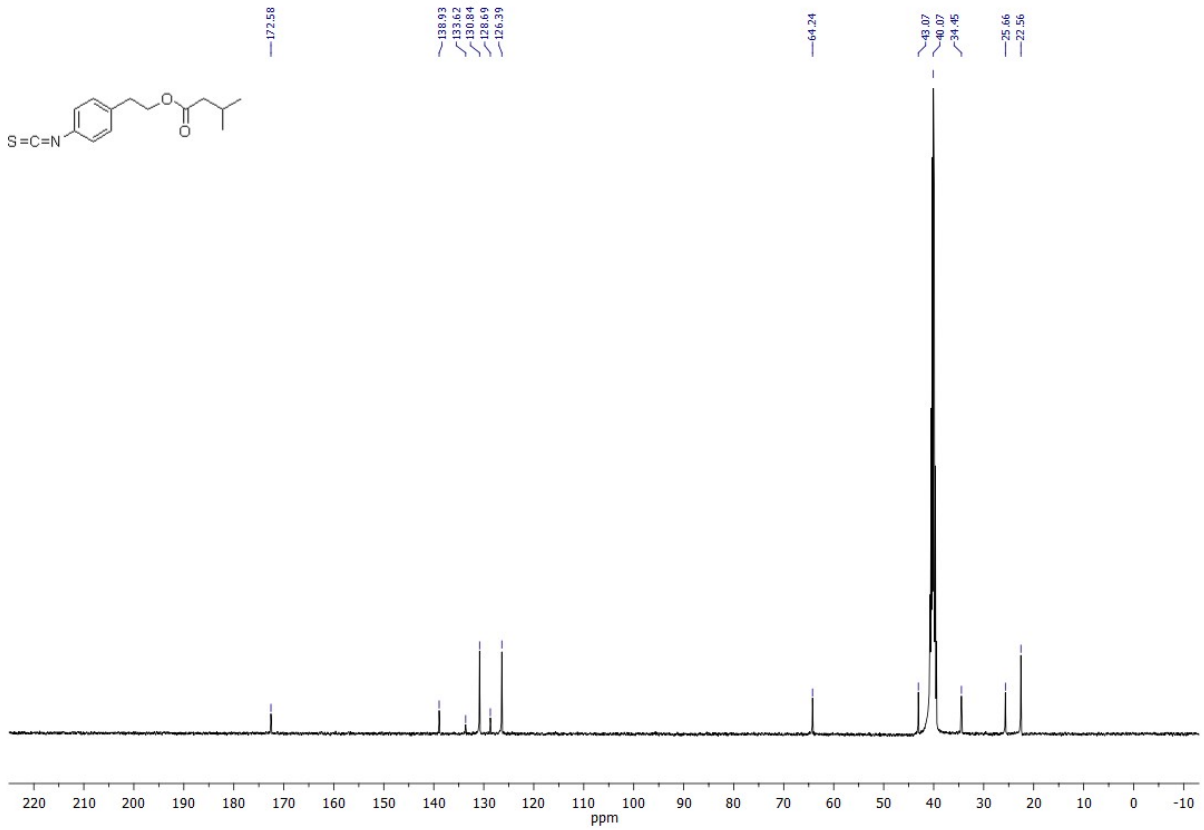

Figure S31. ^{13}C NMR spectra of **I1e**

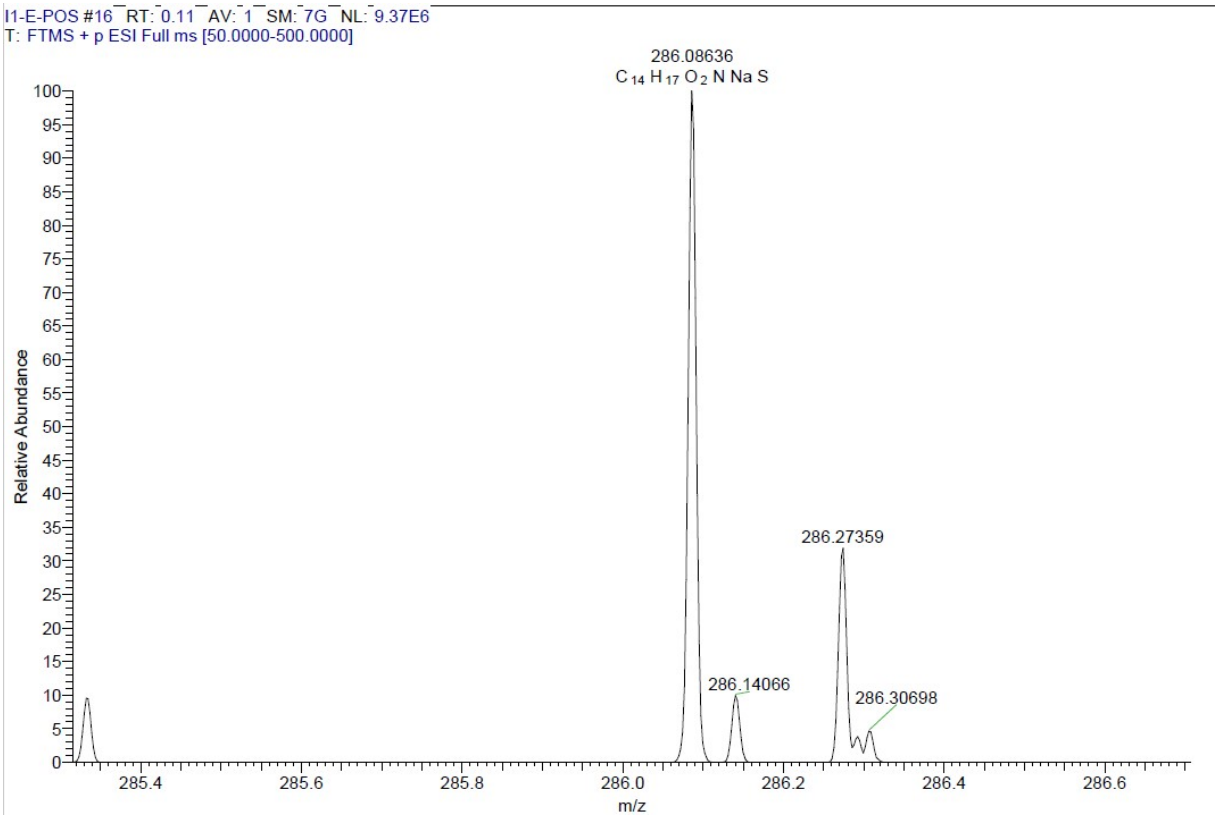

Figure S32. MS spectra of **I1e**

In Silico Results

The ADME properties of all compounds were predicted utilizing the QikProp software (QikProp, version 3.5. New York (NY), Schrödinger LLC, 2012), which evaluates the physicochemical attributes of the isothiocyanate derivatives (Table S1). This tool has the capability to assess the drug-likeness of the ligands in accordance with Lipinski's criteria. All molecules comply with the rule of five. *(C.A. Lipinski, F. Lombardo, B.W. Dominy, P.J. Feeney, Adv. Drug Deliv. Rev.* ***2012****, 64, 4.)*

Table S1. ADME properties of ITC derivatives

Comp.	Chemical formula	MW (g/mol)	Rule of 5	RBN	HBA	HBD	Reactive	BBB, log ratio (TP)	Prot-bind, log t (TP)	Prot-bind, % (TP)	G-LogP (TP)	WSol, log mg/L (TP)
I1	C_9H_9NOS	179.24	OK	3	1	1	R	0.21 (35.83)	-0.37 (35.83)	43.16 (41.51)	2.65	2.92
I2	C_9H_8BrNOS	258.13	OK	3	1	1	R	0.21 (32.62)	-0.37 (32.62)	43.16 (35.94)	2.98	2.67
I3	$C_{10}H_8N_2OS$	204.25	OK	4	2	1	R	0.11 (34.53)	-0.26 (34.53)	35.19 (34.88)	1.27	3.3
I1a	$C_{16}H_{13}NO_2S$	283.35	OK	6	2	0	R	0.27 (53.66)	-0.04 (53.66)	85.54 (35.43)	3.36	1.55
I1b	$C_{17}H_{15}NO_3S$	313.37	OK	7	3	0	R	0.02 (46.81)	-0.09 (46.81)	83.74 (39.46)	3.38	1.08
I1c	$C_{16}H_{12}FNO_2S$	301.34	OK	6	2	0	R	0.27 (48.89)	-0.04 (48.89)	83.57 (41.15)	3.33	1.63
I1d	$C_{16}H_{12}N_2O_4S$	328.34	OK	7	4	0	R	0.27 (51.52)	-0.04 (51.52)	64.45 (35.80)	3.39	1.63
I1e	$C_{14}H_{17}NO_2S$	263.36	OK	7	2	0	R	0.37 (38.73)	-0.18 (38.73)	81.21 (45.93)	3.36	1.76

MW: Molecular weight, **Rule of 5:** Lipinski rule of five, **RBN**: Number of rotatable bonds, **HBA:** Number of hydrogen bond acceptors, **HBD:** Number of hydrogen bond donors, **Reactive:** Reactive groups in molecules, **BBB log ratio:** Blood brain barrier penetration model (Cutoff is -0.3), **Prot-bind log t:** Affinity to human serum albumin, log value of the retention time (Cutoff is 0), **Prot-bind %:** Human serum protein binding (Cutoff is 50%), **G-LogP:** Lipophilicity, log of compound octanol-water distribution (Cutoff is between -0.4 to 5.6), **WSol log mg/L:** Water solubility at 25°C (Cutoff is 2-4).

Table S2. Docking scores of Sulforaphane at the binding pocket of COX-1 and COX-2

Ligands	COX-2 docking score (kcal/mol)	COX-2 ligand effective score (kcal/mol)	COX-1 docking score (kcal/mol)	COX-1 ligand effective score (kcal/mol)
Sulforaphane	-5.050	-0.505	-4.137	-0.414

The Sulforaphane exhibits a docking score of -5.050 kcal/mol against COX-2 and -4.137 kcal/mol against COX-1, indicating a stronger binding affinity to COX-2 compared to COX-1. Moreover, all ITC derivative compounds investigated in our study demonstrated stronger binding to COX targets than Sulforaphane. Although Sulforaphane is known to suppress inflammation, there are no studies or publications in the literature suggesting that it achieves this through direct competitive inhibition by binding to COX targets. Consistent with this, our findings also show that Sulforaphane has low affinity for COX proteins, suggesting that its efficacy may be mediated through downstream pathways rather than direct COX binding.

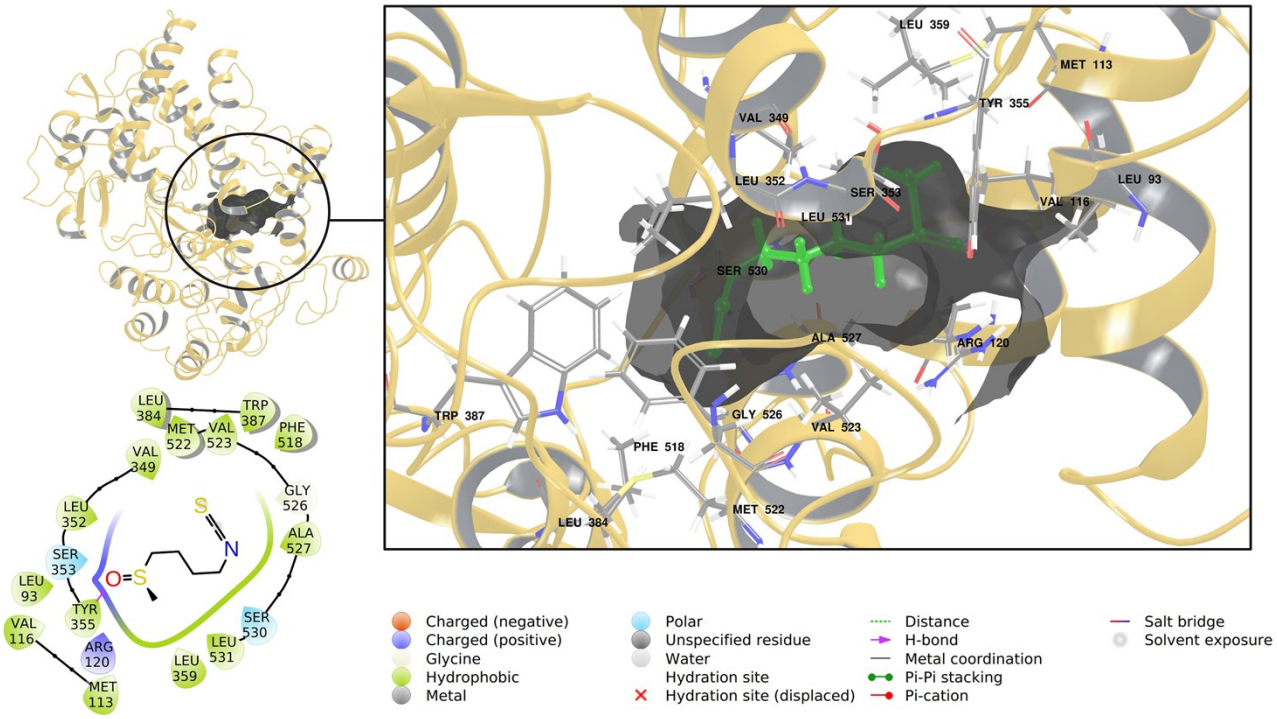

Figure S33. Top-docking pose of the Sulforaphane at binding pocket of human COX-2. 3D and 2D ligand interactions at the binding pocket is focused.